Available online at www.pelagiaresearchlibrary.com

Pelagia Research Library

Advances in Applied Science Research, 2012, 3 (5):2766-2773

ISSN: 0976-8610
CODEN (USA): AASRFC

Thermal and Electrical behaviour of 100 keV N^+ and Ar^+ ion implanted Poly(methyl methacrylate) (PMMA) polymer

Renu Gupta[a*], V. Kumar[a], P. K. Goyal[a], Shyam Kumar[a] and Sneh Lata Goyal[b]

[a]*Department of Physics, Kurukshetra University, Kurukshetra 136119, India*
[b]*Department of Applied Physics, Guru Jambheshwar University of Science and Technology, Hisar 125001, India*

ABSTRACT

Poly (methyl methacrylate) (PMMA) samples were implanted with 100 keV N^+ *and* Ar^+ *ions at fluence upto* $2x10^{16}$ *ions/cm*^{2}*. Ion implantation induced modifications have been observed in the thermal as well as electrical behaviour of PMMA. Thermogravimetric analysis reveals an increase in the thermal stability and hence an increasing trend in the values of thermal degradation energy as a consequence of ion implantation for both the ions has been obtained. Electrical conductivity behaviour shows an increase in the values of conductivity in the implanted samples of PMMA. Structural rearrangements as revealed through FTIR spectroscopy were found to be in strong association with the observed changes in thermal and electrical behaviour of PMMA.*

Keywords: PMMA, ion implantation, activation energy, electrical conductivity, FTIR

INTRODUCTION

In today's era of science and technology, there is a basic need of more and more performing materials. Polymers, in this respect, prove to be excellent engineering materials because of their excellent inherent properties alongwith their tunability by various modes [1-7]. PMMA has emerged as one of the promising material, widely studied and extensively utilized in various applications [8-11]. Owing to its light weight, optical transparency, mechanical strength etc it provides an adequate substance to be utilized in aerospace applications [12-16]. In this arena, PMMA must not only provide excellent mechanical properties but it should also retain its chemical inertness, electrical behaviour after exposure to high levels of radiations. Good thermal stability is also appreciable for polymers to be utilized in various applications.

In the present study, we have emphasized on the modifications produced in the thermal and electrical conductivity behaviour of PMMA as an effect of ion implantation. An attempt has been made to investigate the mechanisms of alterations produced in the polymeric sample due to ion implantation.

MATERIALS AND METHODS

2.1 Sample preparation

The samples (1cm x 1cm) of PMMA (Goodfellow, UK) were cut from a flat sheet of thickness 500 µm and subjected to implantation of 100 keV N^+ and Ar^+ ions using Low Energy Ion Beam Facility (LEIBF) available at Inter University Accelerator Centre (IUAC), New Delhi, India. The irradiation of these samples was performed at room temperature under high vacuum (~10^{-6} torr) upto a maximum dose of $2x10^{16}$ ions/cm^2. The beam current density was kept low in order to avoid thermal degradation during ion implantation. The average projected range of the implanted ions has been found to be 342 nm and 148 nm for N^+ and Ar^+ ion, respectively in PMMA, as calculated using SRIM code (version 2008.04).

2.2 Measurements and characterization

Thermal behaviour has been studied by thermogravimetric analysis using Q600 TA Instrument. Thermograms for the pristine as well as implanted samples were recorded at a linear heating rate of 10°C/min, in the temperature range ~30-600°C.

The DC current voltage measurements of pristine and ion implanted samples of PMMA were carried out in the voltage range 0 to 100 V at room temperature using Keithley 6517 digital programmable electrometer interfaced with computer. In order to ensure good electrical contacts, the samples were silver coated with a certain gap between the two electrodes.

To reveal the structural changes due to ion implantation, the pristine and ion implanted PMMA samples were subjected to FTIR spectroscopic analysis using Shimadzu IR-Affinity-I, FTIR Spectrometer equipped with specular reflectance accessory (Shimadzu, SRM-8000A) and ATR accessory (Pike, ATR-MAX-II with Ge crystal).

RESULTS AND DISCUSSION

3.1 Thermal behavioural studies

3.1.1 Thermogravimetric analysis

Thermogravimetric Analysis (TGA) is a potential means to determine the influence of polymer morphology on thermal stability through the process of thermal degradation. Various kinetic parameters related to the degradation process such as activation energy, frequency factor, free energy of decomposition, entropy of activation, rate coefficient etc. can be obtained using this technique [17-19].

In order to investigate the effect of ion implantation on these kinetic parameters, TGA and DTG thermograms (Figure 1(A) and 1(B)) of the pristine PMMA and TGA thermograms of 100 keV N^+ and Ar^+ ion implanted samples (Figure 2(A) and 2(B)) of PMMA at different ion fluences have been recorded.

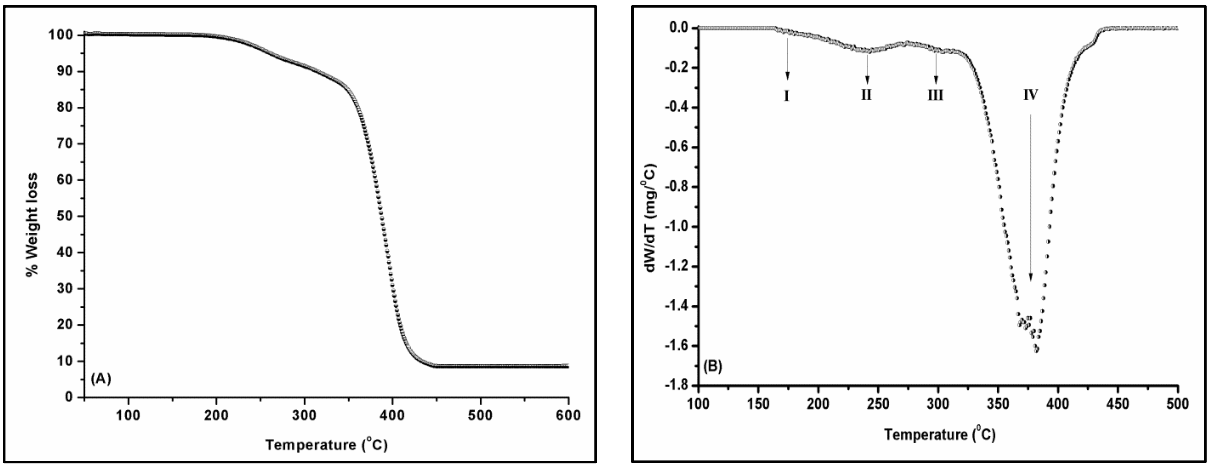

Figure 1: (A) TGA; (B) DTG thermograms of pristine PMMA.

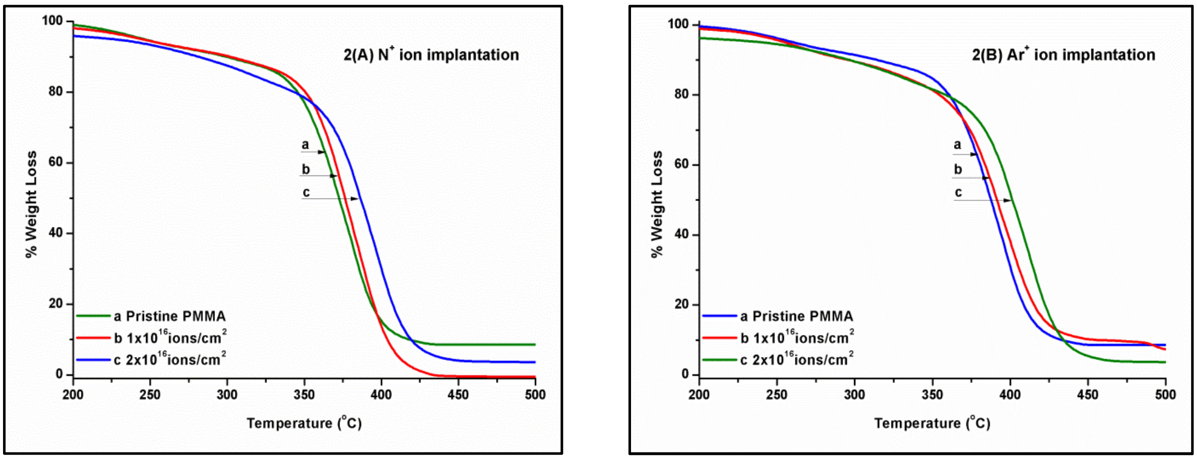

Figure 2: TGA thermograms for (A) N^+ and (B) Ar^+ ion implanted PMMA

It can be clearly seen from figure 1(A) and 1(B) that thermal degradation of pristine PMMA takes place in four steps [20-21] which may be associated to different processes of degradation. The first step falls in the temperature range 0-150°C remains almost stable upto a temperature of 110°C at which initial degradation starts. This is associated with the radical transfer to the unsaturated chain end. The second step in the temperature range 150-230°C and the third step upto a temperature of 320°C may be due to homolytic scission of chains due to H-H bonds and free radical transfer in the unsaturated chain ends, respectively. The second and the third steps are more or less coupled to each other as the hemolytic scissions of the chain may produce free radicals which initiate the third step degradation process. The fourth and the main step of the degradation process extends upto 410°C and is associated with random scissions. Beyond this temperature a residual mass is left out. Figures 2(A) and 2(B) clearly show a gradual increase in the thermal stability of ion implanted samples with increasing ion fluences. It can also be seen that the changes produced are more prominent in the case of N^+ ion implantation as compared to that for Ar^+ ion implantation which can further be confirmed by kinetic analysis.

3.1.2. Kinetic analysis

a) Determination of activation energy

The TGA thermograms have been used to evaluate various kinetic parameters of the degradation reaction by adopting most commonly used method of Horowitz –Metzger [17, 19-27].

The activation energies of pristine and ion implanted samples of PMMA corresponding to the main step of degradation process have been evaluated using the expression [26]

$$ln\left(ln\left(\frac{w_o - w_f}{w - w_f}\right)\right) = \frac{E_a\theta}{RT_s^2} \quad \dots\dots\dots\dots\dots\dots\dots (1)$$

where w_0 is the initial weight, w is the remaining weight at temperature T, w_f is the final weight, E_a is the activation energy, R is gas constant and $\theta = T-T_s$ with T_s as the reference temperature corresponding to $w/w_0 = 1/e$.

The activation energy E_a can be calculated from the slope of the linear fitted line between $\ln(\ln(W_0-W_f / W-W_f))$ and θ as illustrated in Figure 3(A) and 3(B) for N^+ and Ar^+ ion implanted samples respectively, alongwith the pristine sample and these values are tabulated in Table 1.

b) Determination of frequency factor

The corresponding values of frequency factor for the pristine and the ion implanted samples of PMMA have been determined by substituting the values of activation energies in the expression [26]

$$1 = -\frac{A}{\beta}\frac{RT_s^2}{E_a}exp\left(-\frac{E_a}{RT_s}\right) \quad \dots\dots\dots\dots\dots\dots (2)$$

where A is the frequency factor and β is the constant rate of heating.

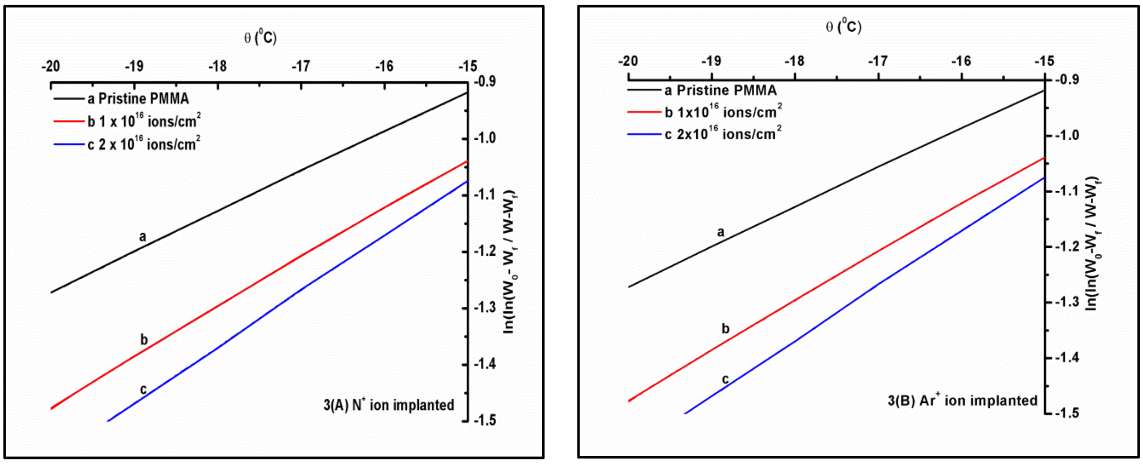

Figure 3: Plots of ln(ln(W_o-W_f/W-W_f)) vs temperature for (A) N^+ and (B) Ar^+ ion implanted PMMA.

The values of frequency factor, so determined for pristine as well as ion implanted samples of PMMA have been enlisted in Table 1. An increasing trend has been observed in the values of activation energy as well as the frequency factor with the increasing ion fluence. Such an increase in the values of activation energy may be attributed to the initialization of cross-linking, possible enhancement in the packing density due to carbonization, compactness, reorganization of molecular arrangements etc. in the polymeric sample which signifies the increase in thermal stability of the polymer. Corresponding to the increase in values of activation energy, the values of frequency factor also increases. Such an increment in the values of frequency factor signifies the enhanced rate of reaction. This may be due to the formation of some interstates as a result of cross-linking or carbonization which increases the reaction rate as an effect of ion implantation [19-23].

The observed values of various kinetic parameters (Table 1) clearly indicate that the extent of changes produced in the case of N^+ implanted PMMA is more pronounced than that produced due to Ar^+ implantation in PMMA. This can be justified by considering the range of these ions in PMMA polymer. As already mentioned, the range of these ions have been found to be 342 nm and 148 nm for N^+ and Ar^+ ion in PMMA respectively, at the same energy (100 keV) of the incident ion. Since N^+ ion has impinged PMMA deeply as compared to Ar^+ ion in the host polymer, hence, the modifications produced due to ion implantation are more prominent in the case of N^+ ion as compared to Ar^+ ion [11-15, 22].

3.2 Electrical studies

3.2.1 DC Conductivity

The current-voltage plots were recorded for pristine as well as N^+ and Ar^+ ion implanted samples of PMMA in the voltage range 0-100V and are presented in figures 4(A) and 4(B), respectively. It can be clearly seen from these figures that the current raises gradually with the increasing ion fluence for both ions. From this data, the surface conductivity of pristine and implanted PMMA samples has been calculated using the relation [28-29] given below and presented in Table 1.

$$\sigma_s = \frac{cosh^{-1}(\frac{d}{2r_o})}{\pi R} \ldots\ldots\ldots\ldots\ldots\ldots (3)$$

where, σs = surface conductivity, d = separation between electrodes, r_0 = radius of the circular electrode, R = resistance measured through the I-V measurements on the implanted surface.

Figure 5 presents the variations in conductivity with respect to the ion fluence for both N^+ and Ar^+ ion implanted samples of PMMA and the corresponding values have been enlisted in table 1.

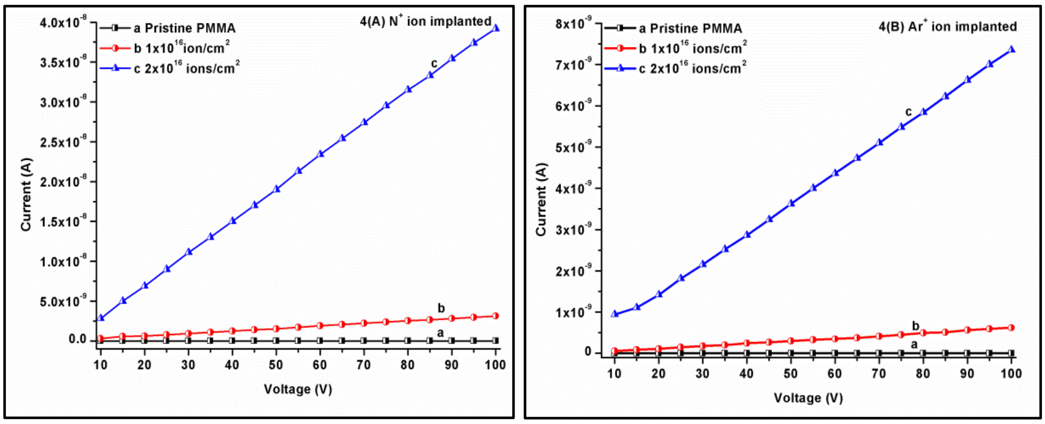

Figure 4: Plots of current vs voltage for (A) N$^+$ and (B) Ar$^+$ ion implanted PMMA.

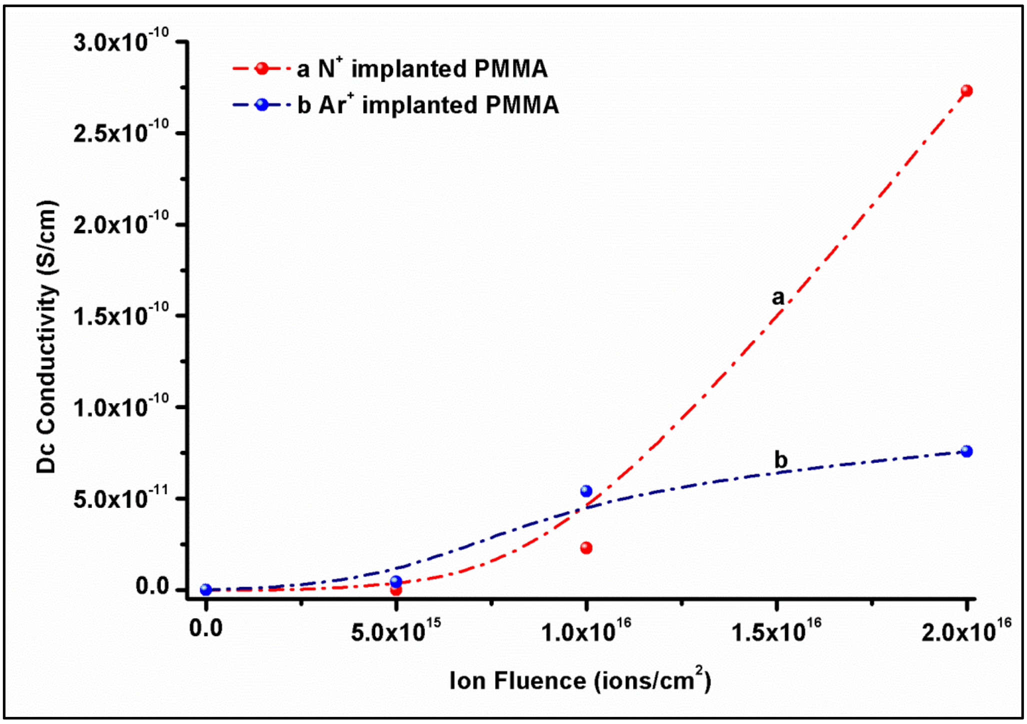

Figure 5: Plots of conductivity vs ion fluence for N$^+$ and Ar$^+$ ion implanted PMMA.

It is clear from figure 5 that initially the conductivity values for N$^+$ and Ar$^+$ ion implanted PMMA are almost of same order upto a dose of 1x10^{16} ions/cm^2 and afterwards, conductivity values for N$^+$ ion implantation rises drastically compared to that for Ar$^+$ ion implantation at ion fluence to 2x10^{16} ions/cm^2. This can be suggested to be due to the large penetration depth of N$^+$ ion as compared to that of Ar$^+$ ion at same energy of incident ion. Further, the observed changes in the conductivity of ion implanted PMMA may be due to the incorporated structural changes as an effect of ion implantation. The possible carbonization, compactness, cross-linkage in the ion implanted PMMA may be responsible for the enhanced conductivity of ion implanted PMMA [28-29]. These structural changes are confirmed through FTIR spectroscopy.

3.3 FTIR Spectroscopy

FTIR spectroscopy is a powerful tool for identifying the bonding structure of polymers. Figure 6 presents the FTIR spectrum of virgin PMMA. It exhibits various peaks at different wavenumbers which may be assigned to different bonding parameters using the available literature [30-32].

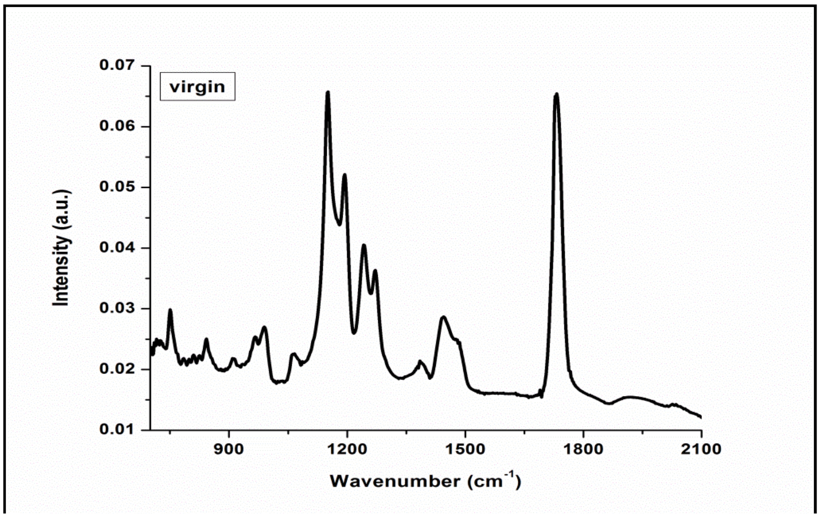

Figure 1: FTIR spectra of virgin PMMA.

The major absorption peak at 1732 cm^{-1} corresponds to the C=Orbital stretching vibrations owing to free carbonyl group present in PMMA. The peaks in the region 1060-1270 cm^{-1} represents C-O-C stretching vibrations. In particular, the peaks at 1066, 1150 cm^{-1} exhibit symmetric C-O-C stretching, while those at 1190, 1242, 1270 cm^{-1} corresponds to antisymmetric C-O-C stretching mode. The smaller peaks in the wavenumber range 910-989 cm^{-1} shows O-CH_3 rocking, while the peak at 842 cm^{-1} is due to CH_2 rocking vibrations. The peak at 752 cm^{-1} may be attributed to C-O bending. All these peaks confirms the monomer structure of PMMA [30-32].

The modifications in the polymeric sample can be clearly observed from the FTIR spectra of N^+ and Ar^+ ion implanted PMMA (figure 7). There is a gradual reduction in the intensities of all the peaks with increasing ion fluence. Some of the peaks in the region (700-1000) cm^{-1} have started dissappearing. All these changes indicate the removal of hydrogen like specices, formation of compact carbonaceous structures etc in the implanted samples of PMMA. All these structural changes support the observed modifications in thermal and electrical behaviour of the polymeric sample as an effect of ion implantation.

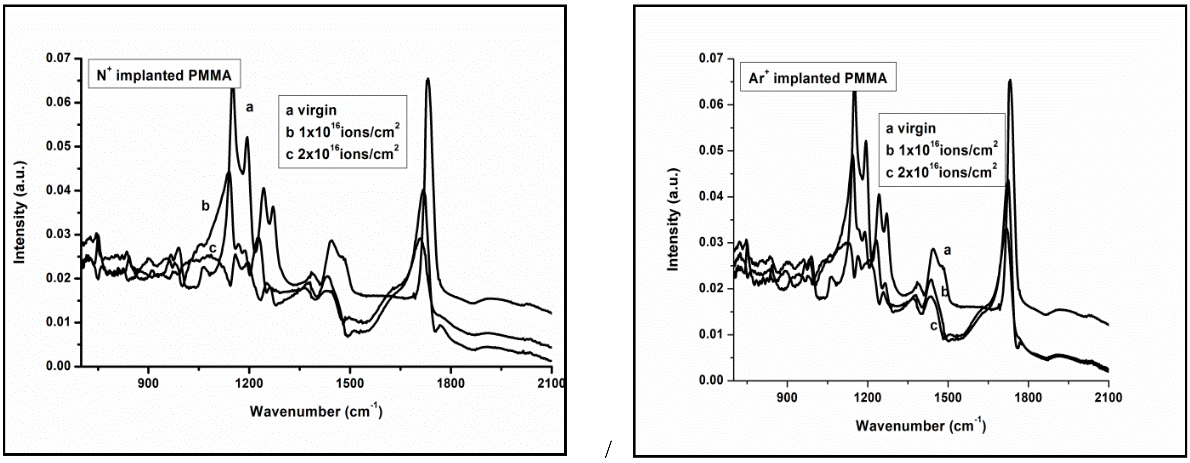

Figure 7: FTIR spectra for N^+ and Ar^+ ion implanted PMMA.

Table 1: List of parameters of thermal stability and electrical conductivity of virgin and ion implanted PMMA.

S. No.	**Ion fluence (ions/cm^2)**	**Activation Energy (kJ/mol)**		**Frequency factor (s^{-1})**		**DC Conductivity (siemen/cm)**	
		N$^+$	**Ar$^+$**	**N$^+$**	**Ar$^+$**	**N$^+$**	**Ar$^+$**
1.	**Virgin**	**224.1**	**224.1**	**5.7E17**	**5.7E17**	**1.1E-14**	**1.1E-14**
2.	**Ix10^{16}**	**259.4**	**249.7**	**1.1E20**	**4.7E19**	**2.3E-11**	**7.6E-11**
3.	**2x10^{16}**	**261.7**	**253.8**	**4.3E20**	**5.1E19**	**2.7E-10**	**5.9E-11**

CONCLUSION

The observed variations in thermal stability and electrical conductivity of ion implanted PMMA may lead to tailor the polymeric sample to suit specific requirments. An increased electrical conductivity of the sample coupled with an enhanced thermal stability as an effect of ion implantation may find extensive applications in various elecronic and opto-electronic devices.

Acknowledgement

The authors are thankful to Dr. D. Kanjilal, IUAC, New Delhi, for valuable discussions. Thanks are due to Dr. P. Kumar, IUAC for helping during irradiation. One of the authors (P.K. Goyal) is thankful to CSIR, New Delhi for financial assistance in form of SRF.

REFERENCES

[1] F. W. Billmeyer Jr. Textbook of Polymer Science; Wiley Interscience: New York (**2005**).
[2] M. F. Zaki J. Phys. D: Appl. Phys. 41 (**2008**), 1754-1758.
[3] E. H. Lee Nucl Instrum Methods B 151 (**1999**), 29-41.
[4] W. Hong, H. J. Woo, H. W. Choi, Y. S. .Kim, G.D. Kim Appl. Surf. Sci. 169-170 (**2001**), 428-432
[5] T. Sharma, S. Aggarwal, A. Sharma, S. Kumar J. Appl. Phys. 102 (**2007**), 063527-1-4.
[6] R. M. Radwan, A. M. Abdul-Kader, A. El-Hag Ali Nucl. Instrum. Methods Phys. Res. B 266 (**2008**), 3588-3594.
[7] D. Fink (*Ed.*), Fundamentals of Ion-Irradiated Polymers, Springer-Verlag, Berlin, Heidelberg, (20**0**4).
[8] S. R. Tatro, G. R. Baker, K. Bisht, J. P. Harmon Polymer 44 (**2003**), 167–176
[9] G.B. Hadjichristov, V. Ivanov, E. Faulques Appl. Surf. Sci. 254 (**2008**), 4820–4827
[10] C. T. Lin, S.W. Kuo, C. F. Huang, F.C. Chang Polymer 51 (**2010**), 883-889.
[11] D. Dorranian, Z. Abedini, A. Hojabri, M. Ghoranneviss J. Non-oxide Glasses 1, 3 (**2009**), 217- 229.
[12] S. W. Kuo, H. C. Kao, F.C. Chang Polymer 44 (**2003**), 6873-6882.
[13] A. V. Leontyev, V. I. Kovalev, A. V. Khomich, F. F. Komarov, V. V. Grigoryev, A. S. Kamishan Micro- and Nanoelect (**2003**), Proceedings of SPIE Vol 5401.
[14] J. R. Kulish, H. Franke, A. Singh, R. A, Lessard, E. J. Knystautas J. Appl. Phys. 63 (**1988**), 2517.
[15] W. He, K. E. Gonsalves, N. Batina, D. B. Poker, E. Alexander, M. Hudson Biomed Microdev 5:2 (**2003**), 101-108.
[16] Y. Koval J. Vac. Sci. Tech. B 22, 2 (**2004**), 843-851.
[17] P. C. Kalsi, K. D. S. Mudher, A. K. Pandey, R.H. Iyer *Thermochimica Acta* **1995**, 254, 331-336.
[18] H. H. G. Jellinek *Aspects of Degradation and Stabilization of Polymers*; Elsevier Scientific Publishing Company : New York, **1978**.
[19] M. F. Zaki, *Brazilian J. Phys.* 38, 4, **2008,** pp558-562.
[20] M. Ferriol, A. Gentilhommea, M. Cocheza, N. Ogetb, J.L. Mieloszynskib *Polymer Degradation and Stability* 79, **2003**, 271–281.
[21] L. E. Manring, D. Y. Sogah, G. M. Cohen. *Macromolecules* **1989**,22:4652–4.
[22] J. H. Flynn, L.A. Wall J. *Research of NBS-A Phy. and Chem.* **1966**, 70A(6), 487-523.
[23] K. G. Mallikarjun *E-Journal of Chem*. **2004**, 1(2), 105-109.
[24] M. R. Rizzatti, M.A. Araujo, R. P. Livi *Nucl. Instrm. And Meth in Phys Res B* 174, **2001**, pp 475-481.
[25] B. K. Singh, P. Kumari, A. Prakash, D. Adhikari *Nature and Science* **2009**, 7(7), 73-78.
[26] H. H. Horowitz, G. Metzger *Anal. Chem.* **1963**, 35(10), 1464-1468.
[27] R. Gupta, V. Kumar, P. K. Goyal, S. Kumar, P.C. Kalsi, S. L. Goyal, *Advances in Applied Science Research,* **2011**, 2 (1): 248-254
[28] P.K. Goyal, V. Kumar, Renu Gupta, S. Mahendia, Anita, S. Kumar *Vaccum* XXX, **2011**, 1-5.

[29] P.K. Goyal, V. Kumar, Renu Gupta, S. Mahendia, T. Sharma, S. Kumar, *Advances in Applied Science Research*, **2011**, 2 (3): 227-231

[30] E. V. Anslyn, D. A. Dougherty *Modern Physical Organic Chemistry*; Edwards Brothers, Inc. USA, **2006**.

[31] D. L. Pavia, G. M. Lampman, G. S. Kriz *Introduction to Spectroscopy 2nd ed.* New York, Harcourt Brace College Publishers, **1994**.

[32] D. Campbell, R. A. Pethric, J. R. White *Polymer Characterization:Physical Techniques* (2nd Ed.) , Stanley Thornes, UK, **2000**